Paper submitted to:
Journal of Alloys and Compounds

TITLE:

A phenomenological investigation on Chlorine intercalated Layered Double Hydroxides used as room temperature gas sensors

AUTHORS:
D. Polese[a], A. Mattoccia[b], F. Giorgi[b], L. Pazzini[a], L. Di Giamberardino[b], G. Fortunato[a], P. G. Medaglia[b]

[a]Istituto per la Microelettronica e Microsistemi - Consiglio Nazionale delle Ricerche, Rome, Italy

[b]Dipartimento Di Ingegneria Industriale, Università degli studi di Roma Tor Vergata, Rome, Italy

Corrispondence to:

Davide Polese, PhD

davide.polese@cnr.it

Doi: https://doi.org/10.1016/j.jallcom.2016.09.125

Abstract

In this paper, a phenomenological study of Layered Double Hydroxide sensing properties respect to common pollutants is presented. Layered Double Hydroxides are a class of nanomaterials characterized by a large surface/volume ratio, able to strongly interact with a wide amount of different chemical compounds. Layered Double Hydroxides materials are also relatively easy to achieve by different synthesis methods on a multiplicity of substrates. Although their characteristics make these materials promising candidates to act as gas sensor, Layered Double Hydroxide gas sensing properties have not still been intensively investigated. To this purpose, a chlorine-intercalated Zn/Al-Layered Double Hydroxide layer is grown by hydrothermal technique on an interdigitated finger array to achieve a resistive gas sensor. The sensing layer has been characterized by Scanning Electron Microscope, X-Ray Diffraction and Energy-Dispersive X-Ray Spectroscopy and then its sensing characteristics have been successfully investigated at room temperature on five common volatile compounds (CO, CO_2, NO, NO_2, CH_4) at six different concentrations. The results demonstrate that Layered Double Hydroxide have interesting properties as low temperature sensing tool for a large range of volatile compounds.

Introduction

Indoor/outdoor air quality monitoring represents a key technology to control the presence of molecules that can be responsible for greenhouse effect and can have a detrimental impact on health and life quality in big cities. Indeed, according to the data of World Health Organization (WHO), the air pollution is one of the main risks to the human health [1]. Therefore, the development of low cost and high sensitivity gas sensors can represent a valuable method to monitor the goodness of the environment and quickly react to the deterioration of the air quality.

In this scenario, several different types of sensors are nowadays available. Among them, solid-state gas sensors are one of the most investigated devices. Their appeal is generally due to the reduced cost of the sensors, high sensitivity and ability to detect a broad range of compounds. In the past years, solid-state gas sensors have implemented a large variety of active materials such as SnO_2, TiO_2, WO_3, ZnO, etc. [2–5] but the requirement of a high working temperature limits their use in low power applications. Although, several techniques have been presented to reduce the power consumption such as nano-structuration of the active material

Doi: https://doi.org/10.1016/j.jallcom.2016.09.125

or take advantage of the high temperature to improve the gas detection [3,6–8], their use in low power application is still challenging. In this work, we introduce another family of material called Layered Double Hydroxides (LDHs) to successfully detect various volatile pollutants at low temperature. In particular, we investigate the sensing characteristics of chlorine-intercalated Zn/Al-LDH nanoplatelets at room temperature.

LDHs, also known as hydrotalcite-like compounds, are a class of ionic lamellar materials belonging to the group of the anionic clays [9]. The natural structure of the material was discovered in the 1842 by Hochstetter and then synthesized for the first time in 1942 by Feitknech [10,11]. In Figure 1, a schematic representation of the LDH structure is shown, the figure reveals the LDH conformation composed of stacked lamellas. Synthetically, the chemical composition of LDH materials can be expressed by the following general formula [9,12]:

$$\left[M_{1-x}^{2+}M_{x}^{3+}(OH)_2\right]_x\left[A^{n-}\right]_{x/n}zH_2O \qquad (1)$$

where, M^{2+} and M^{3+} are two metals (respectively Zn^{2+} and Al^{3+} in our case) and A^{n-} is an anion that is Cl^- in our application. LDHs have a lattice structure formed by stacking positively charged brucite-shaped layers, consisting of a divalent metal ion M^{2+}, octahedrally surrounded by six $(OH)^-$ hydroxyl groups.

The substitution of the M^{2+} metal with a trivalent M^{3+} cation gives rise to the periodic repetition of positively charged sheets (lamellas) alternating with charge-counterbalancing A^{n-} ions that allows the electrostatic neutrality of the brucite layers. This charge displacement produces the possibility of dipole-dipole interactions onto the lamella surfaces, enabling interaction with anions or molecules possessing an electrical dipole. Moreover, inside the interlayer space, water molecules are generally accommodate and a network of hydrogen bonds are present among layers, providing also interacting sites for external molecules. Eventually, it was largely demonstrated the possibility of intercalating different anions in LDH structure [13,14] and changing the anion, it is possible to modify chemical, electronic or optic properties of LDH [12,15]. In this way, at least in principle, the relative response to various volatile compounds could be tuned by means of anion substitution.

Doi: https://doi.org/10.1016/j.jallcom.2016.09.125

LDHs are characterized by a large surface/volume ratio and these structures were proved able to adsorb any kind of atoms/molecules [15,16], indeed, as of their discovery, LDHs materials were used in a very large number of applications ranging from catalysts to drug delivery media, Oxyanion adsorption, etc. [15,17]. Nevertheless, their applications as gas sensors are very limited. The first examples of sensors application adopting LDH is reported in 2006, when Morandi et al. [18] calcinated Zn/Al-LDH to obtain ZnO dust for gas detection and in the same way, Xu et al. [19] in 2013 used LDHs as precursors to obtain composite oxides for gas detection. However, only in 2015, Polese at al. [20] and Sun at al. [21] showed the existence of gas sensing properties of this kind of material. In this paper, we want to provide an accurate phenomenological analysis of the gas sensing properties of one of these materials. To this purpose, several resistive sensors based on Zn/Al-LDHs material have been prepared, characterized by scanning electron microscopy (SEM), X-ray diffraction (XRD) and Energy-Dispersive X-Ray Spectroscopy (EDS) and tested in various atmospheres. The results show that this kind of material is able to detect the tested volatile compounds (CO, CO_2, NO, NO_2 and CH_4) and to discriminate different concentrations at room temperature.

Materials and Methods

Sensors preparation

Resistive sensors based on Zn/Al-LDHs were manufactured by hydrothermal growth on interdigitated fingers array, hereafter called IDA. IDA were designed and fabricated on standard commercial printed circuit board (PCB) with 35 µm thick golden copper track, with the intent of conceiving a device that can be robust and cheap (e.g. prototype production has a price of less 50 euro cent per piece). The starting IDAs are composed of 8 couples of 10 mil (0.254 mm) wide fingers interleaved each other and spaced 10 mil apart. A sensor 3D rendering showing the device dimensions can be observed in Figure 2a.

To prepare the substrates to Zn/Al-LDHs growth, each IDA was progressively cleaned in acetone, isopropyl alcohol and deionized water for 5 mins respectively and finally dried in nitrogen flux. Then, a 200 nm thick layer of Al was deposited on IDA to trigger the following growth mechanism for LDH using a DC magnetron sputtering. The hydrothermal growth of LDHs was carried out by using a nutrient solution composed of a 1:1 ratio of Zinc chloride

Doi: https://doi.org/10.1016/j.jallcom.2016.09.125

($ZnCl_2$) and hexamethylenetetramine ($C_6H_{12}N_4$) at 20 mM concentration [22]. Hexamethylenetetramine was used as a pH regulator to control the solution basicity through the hydrolyzation and release of ammonia at growth temperature [23].

During the growth, the samples were kept in the middle of the solution bottle, anchored to a 45° tilted glass slide in order to avoid any possible contamination. The temperature was fixed at 80°C for 6 hours to promote the LDH nanostructure growth. After the growing time, the samples were removed from the nutrient solution and cooled down in ambient atmosphere. At the end, the samples were washed in ethanol at room temperature to take out some possible precipitate onto the top of the LDHs surface. Figure 2b shows a sensor at the end of the preparation process. Eventually, it is worth to be highlighted that the hydrothermal process allows to grow LDHs on a very large area and it was already demonstrate the possibility of achieve growth on areas larger than 400 cm^2 [24]. In this way, it is possible to prepare several sensors at the same time and potentially at very low cost.

Material characterization

The LDH morphology has been evaluated by SEM: in Figure 3a a SEM image of LDHs grown on IDA layer is shown. In the figure, it is possible to note the typical porous structure of the LDHs, in particular the classical LDH-nanoplatelets that significantly enhance the surface area to volume ratio. To further evidence of the LDH structure, a XRD analysis of the grown LDH layer was performed in addition to an EDS analysis that highlights the elemental composition of the material.

XRD was carried out by using a RIGAKU θ-2θ diffractometer equipped with a Co anode, to generate Co Kα radiation (average value of λ = 1.79206 Å). In Figure 3b, we report the diffraction spectrum of a (Zn/Al) LDH sample with Cl^- intercalated anions, synthesized on a pre-deposited Al coating. Even though only weak diffraction peaks can be achieved due to the random distribution of the LDH-nanopaletes, we are able to deduce the lattice parameters of the LDH hexagonal structure. In detail, from angular positions of 00l reflections, i.e. 003 and 006 peaks, we can calculate an average value of c-axis parameter (corresponding to the thickness of a three stacked basal spacings, see Figure 1) close to 22.70 Å. This experimental result can be used to estimate the value of a lattice parameter (giving the distance between two metal cations in the brucite-like lamella, parameter *a* in Figure 1). In particular, from the angular

Doi: https://doi.org/10.1016/j.jallcom.2016.09.125

position of asymmetrical *hkl* reflections (i.e. having *h* and *k* not simultaneously zero) and by applying the conventional formula for the hexagonal structure, we obtain:

$$\frac{1}{d^2} = \frac{4}{3}\left(\frac{h^2 + hk + k^2}{a^2}\right) + \frac{l^2}{c^2} \quad (2)$$

where *d* is the distance between adjacent (*hkl*) planes, *a* and *c* the lattice parameters. The average values of *a* parameter obtained from 101, 012, 018, 110 and 113 reflections is 3.064 Å. These values (*a* and *c* parameters) are in good agreement with those reported in literature [22,25,26].

To estimate the elemental composition of the sensing layer and in this way verify the presence of Chlorine anion into the LDH structure an EDS analysis is performed. In particular, to highlight the elemental composition of the surface layers, i.e. the LDH layers that mainly interact with the volatile compounds and to avoid the contribution of the underlying bulk structure, the Extra High Tension parameter is set to 5 kV. In Figure 3c, an EDS spectrum is shown, in the figure, it is possible to see the peaks corresponding to Zinc, Aluminum, Chlorine and Oxigen. The peaks recognition has been performed with Inca suite software [27] that has been also used to perform a quantitative elemental analysis of LDHs surface. In Table 1 the estimated content of the found elements is reported. These results confirm the presence of the Chlorine in our sample. Finally, it is important to note that the Zinc/Aluminium ratio is 3:1, this result is in agreement with LDHs literature [28,29].

Experimental setup

The prepared sensors were placed in a customized sealed chamber with tube fittings for gas inlet and outlet. The chamber was endowed of a particular shield, above the sensors accommodation, to permit a homogenous distribution of the gas mixture under test and avoiding a direct flow on the samples. A mass flow system controlled by PC was used to control the flux through the chamber. During the measurements, a constant flux of 200 sccm was fixed by the mass flow system that also sets the dilution factors of the testing gases.

Doi: https://doi.org/10.1016/j.jallcom.2016.09.125

Each concentration was obtained diluting in nitrogen carbon monoxide (CO), carbon dioxide (CO_2), nitric oxide (NO), nitrogen dioxide (NO_2), and methane (CH_4) concentrations measured from certified bottles where they were diluted in pure nitrogen. For each compound, the same dilution factors were applied and the resulting concentrations are shown in Table 2. Nitrogen was chosen as carrier gas since we did not observe significant differences in the measurements with dry air carrier and these results can be compared more easily with others reported in literature. The sensors were exposed for 60 s to six increasing concentrations and then cleaned in wet nitrogen for 500 s. During the whole measurements the humidity was kept constant to 50% RH fluxing 100 sccm of pure nitrogen through a gas bubbler containing deionized water. The RH level was maintained constant to avoid the possible change of the LDH inter-lamellar content of water. Finally, every volatile compound was measured in triplicate at room temperature (approximately 22°C) and the DC sensor resistances were measured by means of an Agilent 34401a multimeter connected to PC.

Results and discussion

To investigate the sensor characteristics, a set of key parameters have been taken into account such as sensitivity and selectivity [30,31]. To this purpose, several sensors were exposed to diverse volatile compounds at different concentrations in order to evaluate the above-mentioned parameters. In particular, each sensor was randomly exposed to the five volatile compounds at six increasing concentrations at room temperature.

Gas measurements

As first experiment, we studied the behavior of the sensing material increasing the content of water in the nitrogen flux. In fact, the LDHs are particularly sensitive to the specific humidity range in which operates. We found out that the value of the resistance of all the samples tends to constantly increase in a pure nitrogen flux due to the dehydration of the nanostructures that change also in the morphology. This effect is reversible and after few hours in nitrogen enriched with deionized water, the samples resistance value decreases again towards the initial value.

Doi: https://doi.org/10.1016/j.jallcom.2016.09.125

As can be seen in Figure 4, also the specific response to a known concentration changes if we choose to work at a different humidity value. Again, this suggests that the presence of water inside the porous structure also plays a crucial role probably decreasing the active sites of the sensor, thus minimizing the response of the sample. To make a fair comparison among the different analytes, we decided to measure the samples with a constant value of humidity of 50% RH.

In order to evaluate the selectivity and sensitivity of LDH sensors, several samples were exposed to six concentrations of five volatile compounds (namely CO, CO_2, NO, NO_2 and CH_4). In Figure 5a, the measured sensor resistance for a complete sequence of concentrations of CH_4 (taken as an example) is shown. Even if a slight linear drift appears, this does not invalidate the measurements. Indeed, the sensor response variation or the sensor relative variation shown in figure 6 or figure 7 respectively shown consistent responses that are almost not affected by drift.

Figure 5b shows a detail of two consecutive concentrations (namely 62 and 125 ppm) of CO, where it is possible to appreciate also the recovery time of the sensors, which is less than 100 s. Finally, Figure 6a-e show the typical sensor response to the different concentrations of the tested gases: CO, CO_2, NO_2, CH_4, NO respectively. For each concentration, three repetitions are shown. Comparing the sensor response to the compounds, it is important to note the different shapes of the sensor responses to the different compounds and the different time of sensing. These differences are probably due to the peculiar processes of absorption or possible reactions onto the sensor surfaces, hypothesis that need a more accurate investigation. It must also be pointed out that for the highest concentration in some compounds an initial increase of the resistance is observed. This trend that seems to present an inverse behavior is probably due to a temporary poisoning of the sensor. However, this effect does not affect the following measurements.

To summarize the results, the relative variation of the sensor response $\frac{R-R_0}{R_0}$ has been calculated, where *R* is the minimum dc resistance of the sensor during the gas exposure and R_0 is the dc resistance of the gas sensor in the wet nitrogen just before the gas exposure. Figure 7 shows the sensor response to the different compounds, the standard deviation puts in

Doi: https://doi.org/10.1016/j.jallcom.2016.09.125

evidence the repeatability of the sensor response along the three repetitions. Indeed, in this case the standard deviation takes into account the variation of the sensor response to distinct exposures of the same atmosphere, i.e. volatile compound and concentration. In this way, the short-term stability of the sensor is also highlighted, whereas, a long-term stability analysis is outside of the aim of this work and will be taken into account in future works.

The sensor response data, showed in Figure 7, have been fitted with the classical power law for semiconductor gas sensors [32] relation that is also in agreement with the results of Sun at al. [21].

$$R([c]) = a \cdot [c]^b + d \tag{3}$$

where the parameter a, b and d are the fitting parameters and c is the concentration of the compound taken into consideration. The fitting are performed in MATLAB and the resulting profiles are shown in Figure 7 too, showing a good agreement with the experimental data, (R^2 parameter greater than 0.9090 for all fittings). The values obtained for the different volatile compounds are listed in Table 3.

The reckoned power law curves are used to estimate the sensitivity, according to D'Amico et al. [31] as the derivative of the sensor response:

$$S(c) = \frac{\partial R(c; gas, H,\ T,\ P \ldots)}{\partial c} = ab[c]^{b-1} \tag{4}$$

In Figure 8 the specific sensitivity to each compound is reported. As can be seen for almost all analytes, the trends are similar as expected for Langmuir-like adsorption while for NO_2, the sensitivity shapes suggests a different interaction with the LDH material.

Finally, in Figure 9 the comparison among the sensor responses to the middle scale concentration of the different compounds are shown. This comparison clearly shows the un-selectivity of this kind of sensors. We believe that by changing the specific intercalated ion into the LDH matrix, it will be possible to discriminate an increasing number of volatile compounds

Doi: https://doi.org/10.1016/j.jallcom.2016.09.125

with different cross sensitivities, by using the same low cost and low working temperature material.

The results highlight that sensors based on this LDH material permit to detect all the five gases for a wide range of concentrations. Moreover, the LDH materials have shown an intrinsic ability to respond to the various volatile compounds and require the maintenance of a certain hydration. However, due to the very few studies on sensor applications of these materials and the few available experimental data, the sensing mechanisms are still not clear and only some assumptions on them can be done. In our opinion, several interaction mechanisms work together to produce the sensor response. How it was previously described, the presence of hydrogen bonds among layers makes available interacting sites, and the charge displacement between LDH lamellas can produce dipole-dipole interaction but in our opinion these processes assist a dissociative gas sensing effect onto or into firsts lamellas of the LDH surface that let the sensor working as a pH sensor [33]. Clearly, a definitive conclusion needs more focused investigations.

Conclusions

In conclusion, the use of LDH material as gas sensor at room temperature has been demonstrated. In particular, the sensing properties of the chlorine intercalated LDHs have been shown. Several resistive sensors based on this material have been fabricated, characterized by SEM, XRD and EDS analysis and then successfully tested in the detection of five volatile compounds (CO, CO_2, NO, NO_2 and CH_4) at controlled values of humidity. Under these conditions, the sensors have shown the capability of distinguishing several concentrations with a very good short-term stability. This kind of material appears very interesting in gas sensor applications for its ability of detecting various pollutant volatile compounds at room temperature without the requirements of a heating element. Some possible sensing mechanisms has been identified and they will be the aim of further studies.

Doi: https://doi.org/10.1016/j.jallcom.2016.09.125

References

[1] WHO, World Health Organization, http://www.who.int/mediacentre/factsheets/fs313/en/.

[2] E. Kanazawa, G. Sakai, K. Shimanoe, Y. Kanmura, Y. Teraoka, N. Miura, et al., Metal oxide semiconductor N2O sensor for medical use, Sensors Actuators B Chem. 77 (2001) 72–77. doi:10.1016/S0925-4005(01)00675-X.

[3] I. Simon, N. Bârsan, M. Bauer, U. Weimar, Micromachined metal oxide gas sensors: Opportunities to improve sensor performance, Sensors Actuators, B Chem. 73 (2001) 1–26. doi:10.1016/S0925-4005(00)00639-0.

[4] K. Wetchakun, T. Samerjai, N. Tamaekong, C. Liewhiran, C. Siriwong, V. Kruefu, et al., Semiconducting metal oxides as sensors for environmentally hazardous gases, Sensors Actuators B Chem. 160 (2011) 580–591. doi:10.1016/j.snb.2011.08.032.

[5] K. Galatsis, Y.X. Li, W. Wlodarski, E. Comini, G. Sberveglieri, C. Cantalini, et al., Comparison of single and binary oxide MoO3, TiO2 and WO3 sol-gel gas sensors, Sensors Actuators, B Chem. 83 (2002) 276–280. doi:10.1016/S0925-4005(01)01072-3.

[6] E. Martinelli, D. Polese, A. Catini, A. D'Amico, C. Di Natale, Self-adapted temperature modulation in metal-oxide semiconductor gas sensors, Sensors Actuators B Chem. (2011).

[7] J. Courbat, D. Briand, L. Yue, S. Raible, N.F. de Rooij, Drop-coated metal-oxide gas sensor on polyimide foil with reduced power consumption for wireless applications, Sensors Actuators B Chem. 161 (2012) 862–868. doi:10.1016/j.snb.2011.11.050.

[8] J. Fonollosa, L. Fernández, R. Huerta, A. Gutiérrez-Gálvez, S. Marco, Temperature optimization of metal oxide sensor arrays using Mutual Information, Sensors Actuators B Chem. 187 (2013) 331–339. doi:10.1016/j.snb.2012.12.026.

[9] Q. Wang, D. O'Hare, Recent Advances in the Synthesis and Application of Layered Double Hydroxide (LDH) Nanosheets, Chem. Rev. 112 (2012) 4124–4155. doi:10.1021/cr200434v.

[10] J.J. Bravo-suarez, E. Paez-mozo, S.T. Oyama, Review of the synthesis of layered double hydroxides: A thermodynamic approach, Quim. Nov. 27 (2004) 601–614. doi:10.1590/S0100-40422004000400015.

[11] M. Hadnadjev, T. Vulic, R. Marinkovic-Neducin, Y. Suchorski, H. Weiss, The iron oxidation state in Mg-Al-Fe mixed oxides derived from layered double hydroxides: An XPS study, Appl. Surf. Sci. 254 (2008) 4297–4302. doi:10.1016/j.apsusc.2008.01.063.

[12] A.I. Khan, D. O'Hare, Intercalation chemistry of layered double hydroxides: recent developments and applications, J. Mater. Chem. 12 (2002) 3191–3198. doi:10.1039/b204076j.

[13] S. V. Krivovichev, Minerals as Advanced Materials II, 2012.

[14] A. Fahami, F.S. Al-Hazmi, A.A. Al-Ghamdi, W.E. Mahmoud, G.W. Beall, Structural characterization of chlorine intercalated Mg-Al layered double hydroxides: A comparative study between mechanochemistry and hydrothermal methods, J. Alloys Compd. 683 (2016) 100–107. doi:10.1016/j.jallcom.2016.05.032.

[15] K.H. Goh, T.T. Lim, Z. Dong, Application of layered double hydroxides for removal of oxyanions: A review, Water Res. 42 (2008) 1343–1368. doi:10.1016/j.watres.2007.10.043.

[16] F.L. Theiss, S.J. Couperthwaite, G.A. Ayoko, R.L. Frost, A review of the removal of anions and oxyanions of the halogen elements from aqueous solution by layered double hydroxides, J. Colloid Interface Sci. 417 (2014) 356–368. doi:10.1016/j.jcis.2013.11.040.

Doi: https://doi.org/10.1016/j.jallcom.2016.09.125

[17] F. Mills, S. J., Christy, A. G., Génin, J. M., Kameda, T., & Colombo, Nomenclature of the hydrotalcite supergroup: natural layered double hydroxides. Mineralogical Magazine, Mineral. Mag. 76 (2012) 1289–1336.

[18] S. Morandi, F. Prinetto, M. Di Martino, G. Ghiotti, O. Lorret, D. Tichit, et al., Synthesis and characterisation of gas sensor materials obtained from Pt/Zn/Al layered double hydroxides, Sensors Actuators, B Chem. 118 (2006) 215–220. doi:10.1016/j.snb.2006.04.025.

[19] Q.-H. Xu, D.-M. Xu, M.-Y. Guan, Y. Guo, Q. Qi, G.-D. Li, ZnO/Al2O3/CeO2 composite with enhanced gas sensing performance, Sensors Actuators B Chem. 177 (2013) 1134–1141. doi:http://dx.doi.org/10.1016/j.snb.2012.12.029.

[20] D. Polese, A. Mattoccia, F. Giorgi, L. Pazzini, A. Ferrone, L. Di Giamberardino, et al., Layered Double Hydroxides Intercalated with Chlorine Used as Low Temperature Gas Sensors, Procedia Eng. 120 (2015) 1175–1178. doi:10.1016/j.proeng.2015.08.765.

[21] H. Sun, Z. Chu, D. Hong, G. Zhang, Y. Xie, L. Li, et al., Three-dimensional hierarchical flower-like Mg–Al-layered double hydroxides: Fabrication, characterization and enhanced sensing properties to NOx at room temperature, J. Alloys Compd. 658 (2016) 561–568. doi:10.1016/j.jallcom.2015.10.237.

[22] D. Scarpellini, C. Leonardi, A. Mattoccia, L. Di Giamberardino, P.G. Medaglia, G. Mantini, et al., Solution-Grown Zn / Al Layered Double Hydroxide Nanoplatelets onto Al Thin Films : Fine Control of Position and Lateral Thickness, 2015 (2015) 1–9.

[23] K.M. McPeak, T.P. Le, N.G. Britton, Z.S. Nickolov, Y. a. Elabd, J.B. Baxter, Chemical bath deposition of ZnO nanowires at near-neutral pH conditions without hexamethylenetetramine (HMTA): Understanding the role of HMTA in ZnO nanowire growth, Langmuir. 27 (2011) 3672–3677. doi:10.1021/la105147u.

[24] A. Mattoccia, E. Bernardone, L. Digiamberardino, P. Gaudio, A. Malizia, A. Orsini, et al., Rivestimenti Studio morfologico di nanostrutture di Layered Double Hydroxides (LDH) depositate su film sottili di alluminio Memorie, (2015) 15–22.

[25] D. Scarpellini, C. Falconi, P. Gaudio, A. Mattoccia, P.G. Medaglia, A. Orsini, Microelectronic Engineering Morphology of Zn / Al layered double hydroxide nanosheets grown onto aluminum thin films, Microelectron. Eng. 126 (2014) 129–133. doi:10.1016/j.mee.2014.07.007.

[26] G.M. Lombardo, G.C. Pappalardo, F. Costantino, U. Costantino, M. Sisani, Thermal Effects on Mixed Metal (Zn / Al) Layered Double Hydroxides : Direct Modeling of the X-Ray Powder Diffraction Line Shape Through Molecular Dynamics Simulations, Chem. Mater. 20 (2008) 5585–5592. doi:10.1021/cm801053d.

[27] Inca Suite Software http://www.oxford-instruments.com.

[28] M.S. Yarger, E.M.P. Steinmiller, K. Choi, Electrochemical Synthesis of Zn - Al Layered Double Hydroxide (LDH) Films, Inorg. Chem. 47 (2008) 5859–5865.

[29] F.L. Theiss, G.A. Ayoko, R.L. Frost, Synthesis of layered double hydroxides containing Mg2+, Zn2+, Ca2+ and Al3+ layer cations by co-precipitation methods—A review, Appl. Surf. Sci. 383 (2016) 200–213. doi:10.1016/j.apsusc.2016.04.150.

[30] N. Barsan, D. Koziej, U. Weimar, Metal oxide-based gas sensor research: How to?, Sensors Actuators, B Chem. 121 (2007) 18–35. doi:10.1016/j.snb.2006.09.047.

[31] A. D'Amico, C. Di Natale, A contribution on some basic definitions of sensors properties, IEEE Sens. J. 1 (2001) 183–190. doi:10.1109/JSEN.2001.954831.

[32] N. Yamazoe, K. Shimanoe, Theory of power laws for semiconductor gas sensors, Sensors Actuators B

Doi: https://doi.org/10.1016/j.jallcom.2016.09.125

Chem. 128 (2008) 566–573. doi:10.1016/j.snb.2007.07.036.

[33] A. Helwig, G. Müller, G. Sberveglieri, M. Eickhoff, On the low-temperature response of semiconductor gas sensors, J. Sensors. 2009 (2009). doi:10.1155/2009/620720.

Figure Captions

Figure 1 A schematic representation of the LDH structure is shown. In the figure, the atomic species assembling the nanostructructure are highlighted. In particular, it is possible to note how the octaedrically surrounded metallic atoms shape the lamellas and how stacked lamellas form the LDH plates. Moreover, the figure shows the cell parameters (a and c) calculated by XRD analysis.

Figure 2 a) A 3D rendering of the interdigitated finger. b) An interdigitated finger structure covered by LDH layer.

Figure 3 a) A SEM image of the LDH structure growth on the interdigitated finger. The image shows LDH-nanoplateles and how their arrangement form the characteristic porous structure of LDH. b) XRD spectrum of LDH structure is shown, in the figure the reticular peaks are labeled. c) EDS spectrum of LDHs surface the peak labeling is performed by INCA suite version 4.15 Oxford Instrument. Extra High Tension is set to 5kV to avoid the bulk contribution and highlight the elemental composition of the surface composed of LDH nano-plateles.

Figure 4 Sensor response to 125 ppm of CO_2 at different RH values (namely 30%, 50% and 70%) is shown. It is possible to note how the aqueous content inside the porous structure of LDHs play a role in the sensing mechanism of the material changing the sensor response.

Figure 5 a) Sensor response to the full sequence of concentrations of methane. In the figure is pointed out the different concentrations; only the first repetition is highlighted. Each gas exposure is followed by a cleaning in wet nitrogen. b) A detail of the sensor response for two consecutive concentrations of CO (62 and 125 ppm) is shown; the gas exposure is highlighted in blue. From the figure it is possible to appreciate a recovery time of roughly 100 s.

Figure 6 Normalized sensor response variation to the different volatile compounds. Each concentration has been measured in triplicate. a) CO, b) CO_2, c) NO_2, d) CH_4, e) NO. The different concentrations for each compound are listed in table 2.

Figure 7 Sensor response fittings. In figure, the fitting curve obtained for the experimental data presented in figure 6 are shown.

Figure 8 The plot shows the specific sensitivity of the LDH device to each detected compound.

Figure 9 Sensor response to middle scale concentration (i.e. approximately 125 ppm for all compounds) to the different volatile compounds under test. The figure puts in evidence the unselective characteristics of this kind of sensors.

Doi: https://doi.org/10.1016/j.jallcom.2016.09.125

Doi: https://doi.org/10.1016/j.jallcom.2016.09.125

Table Captions

Table 1 EDS quantitative element analysis performed with INCA suite version 4.15 Oxford Instrument on the EDS spectrum of figure 3c. A Zinc/Aluminium ratio of 3:1 can be appreciated, this result is in agreement with LDHs literature.

Table 2 The concentrations of the measured compounds are listed.

Table 3 The fitting parameters for the different compounds are shown. Moreover, the parameter R^2 of the fittings is reported.

Doi: https://doi.org/10.1016/j.jallcom.2016.09.125

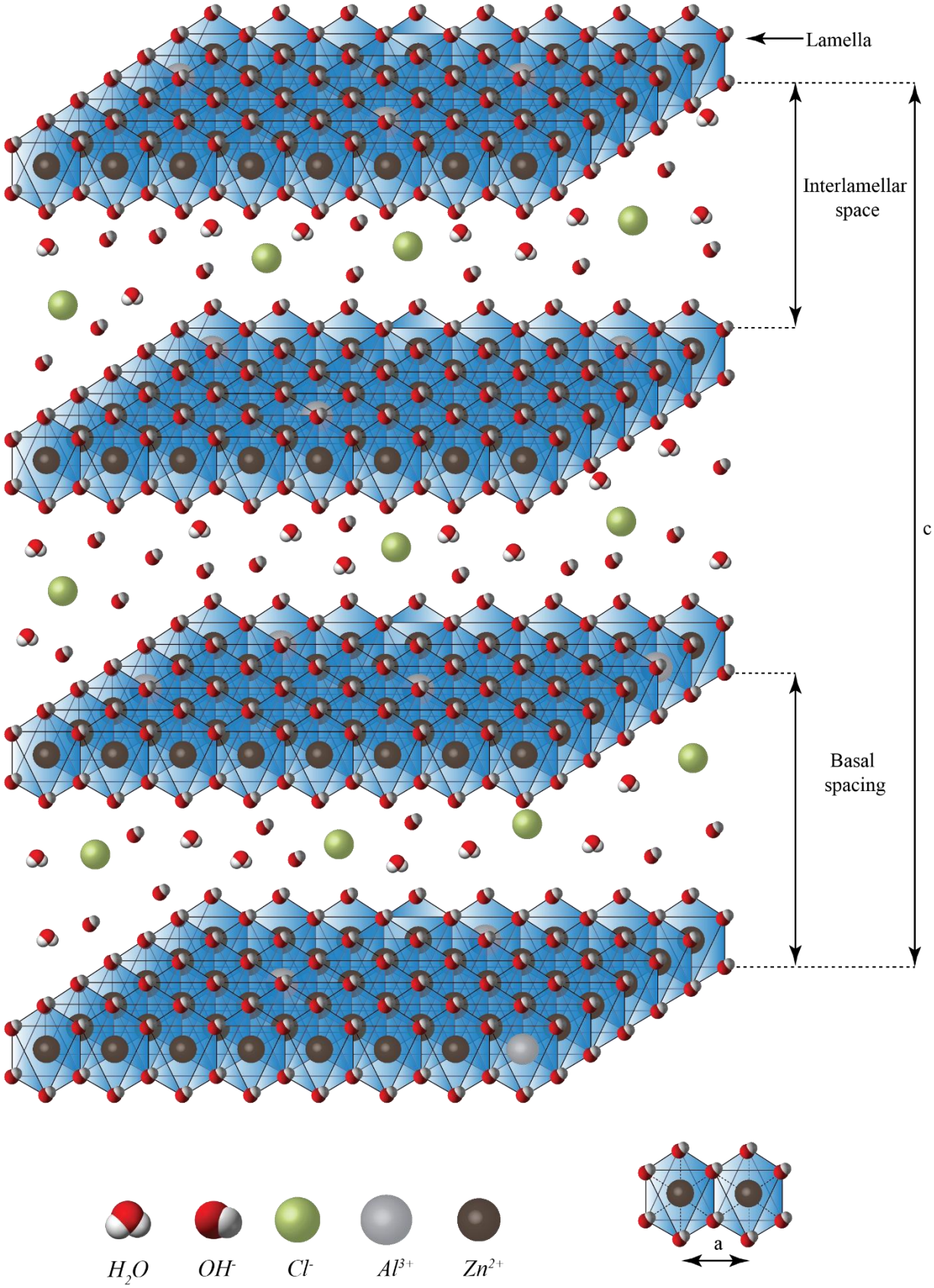

Doi: https://doi.org/10.1016/j.jallcom.2016.09.125

Figure 1

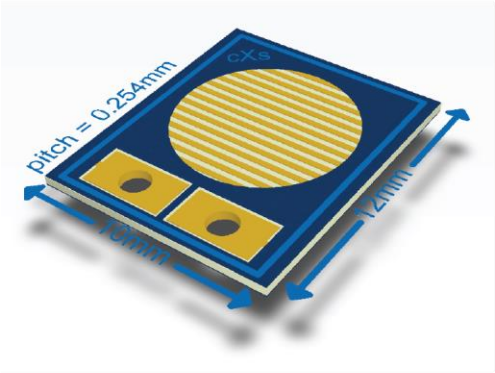

a)

b)

Figure 2

Doi: https://doi.org/10.1016/j.jallcom.2016.09.125

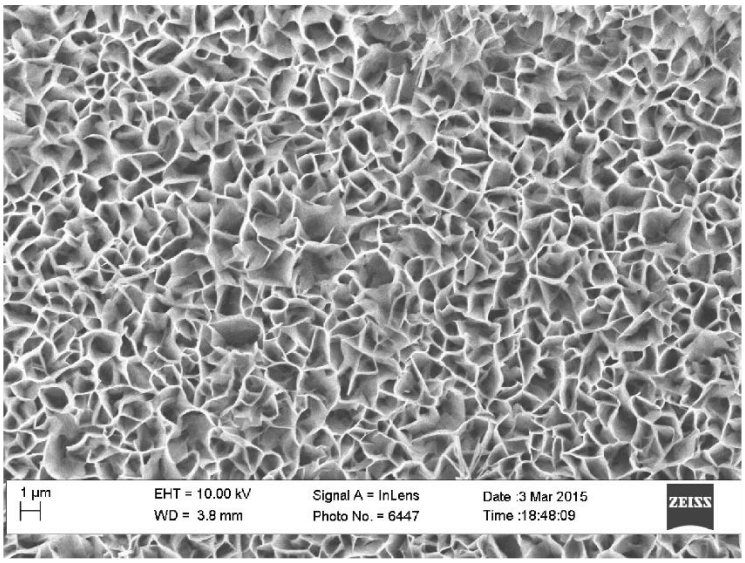

a)

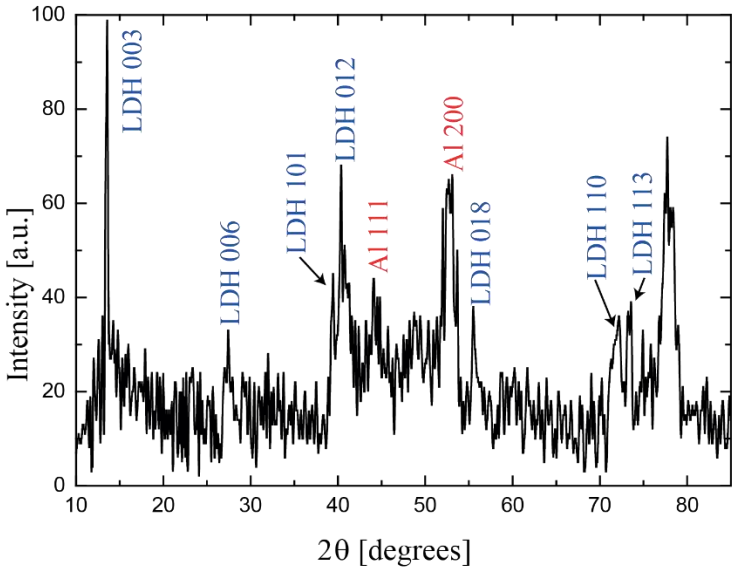

b)

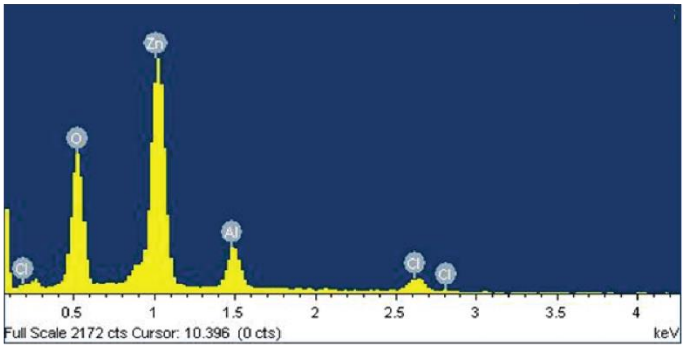

c)

Doi: https://doi.org/10.1016/j.jallcom.2016.09.125

Figure 3.

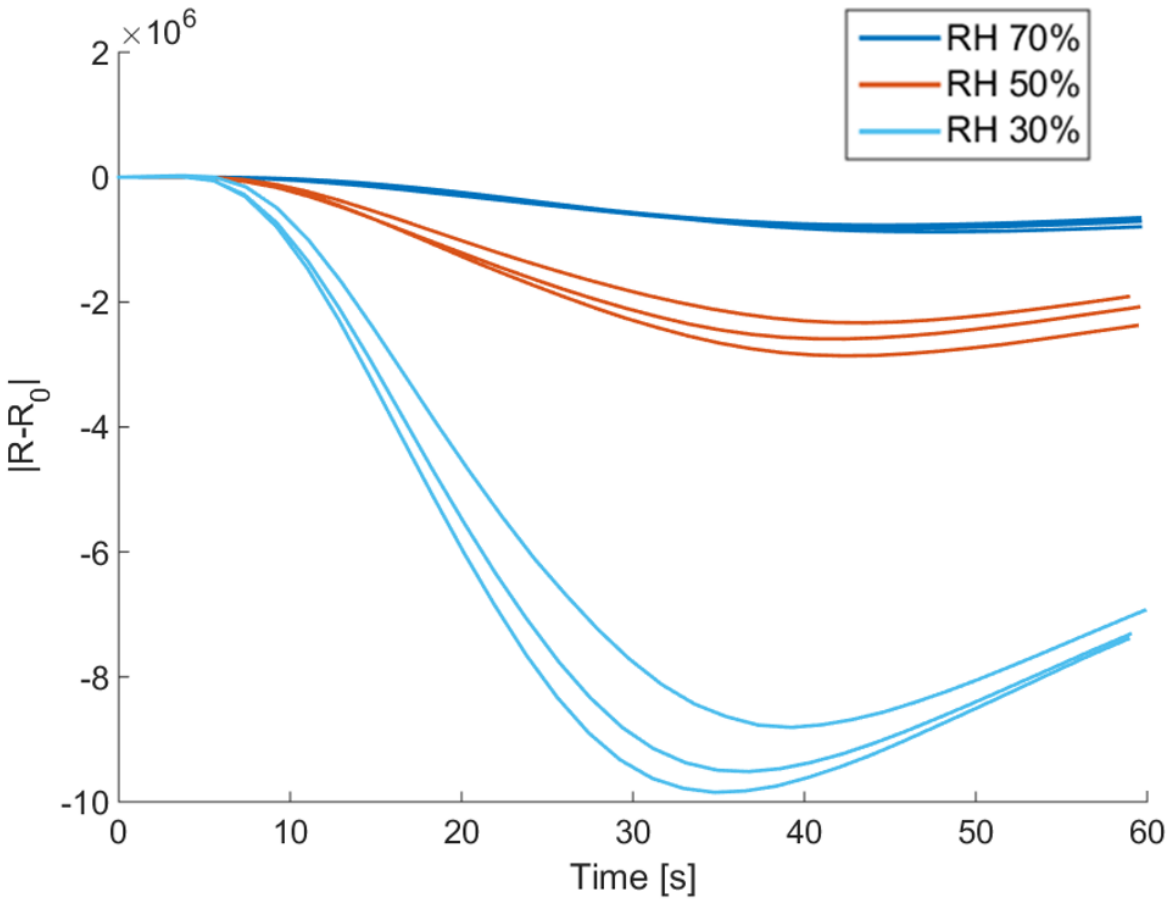

Figure 4

Doi: https://doi.org/10.1016/j.jallcom.2016.09.125

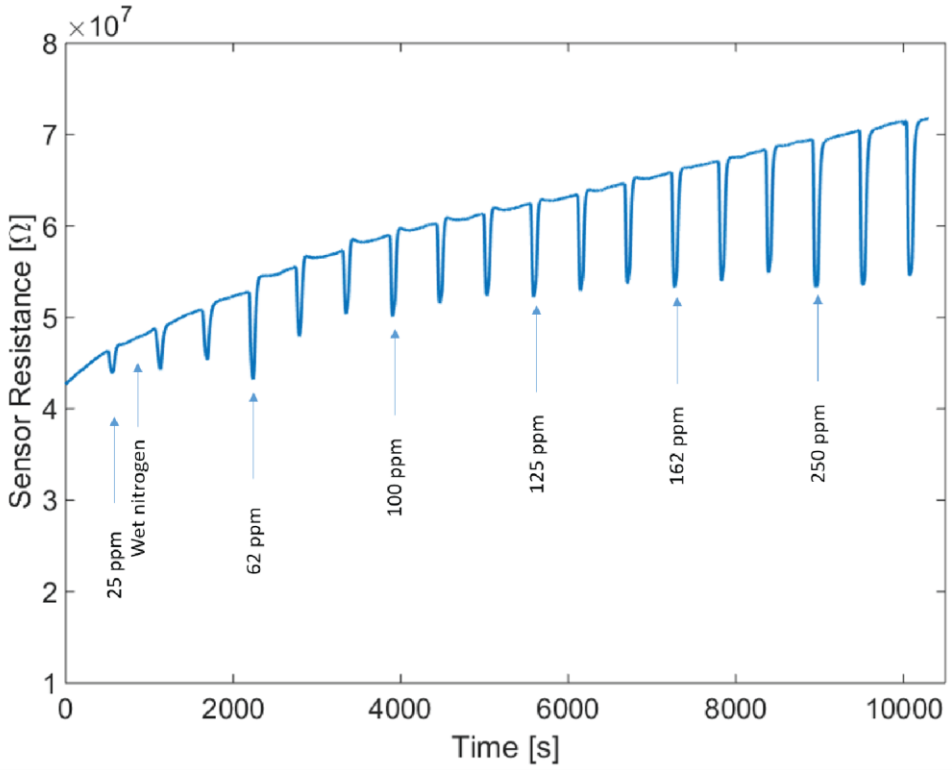

a)

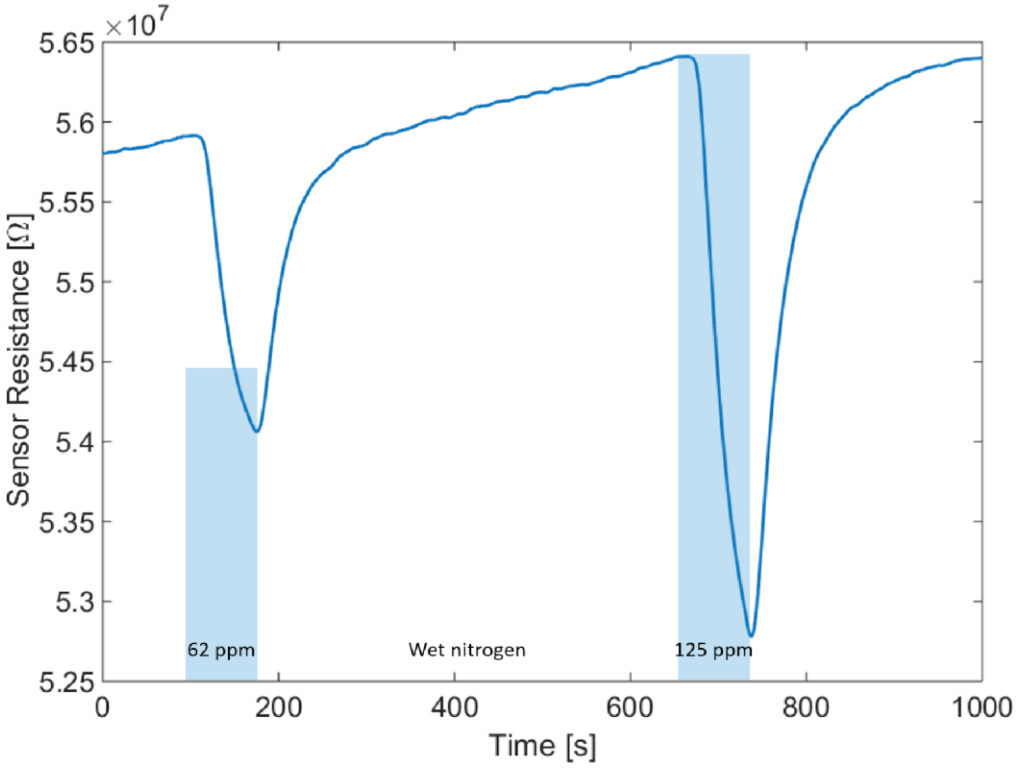

b)

Doi: https://doi.org/10.1016/j.jallcom.2016.09.125

Figure 5

Doi: https://doi.org/10.1016/j.jallcom.2016.09.125

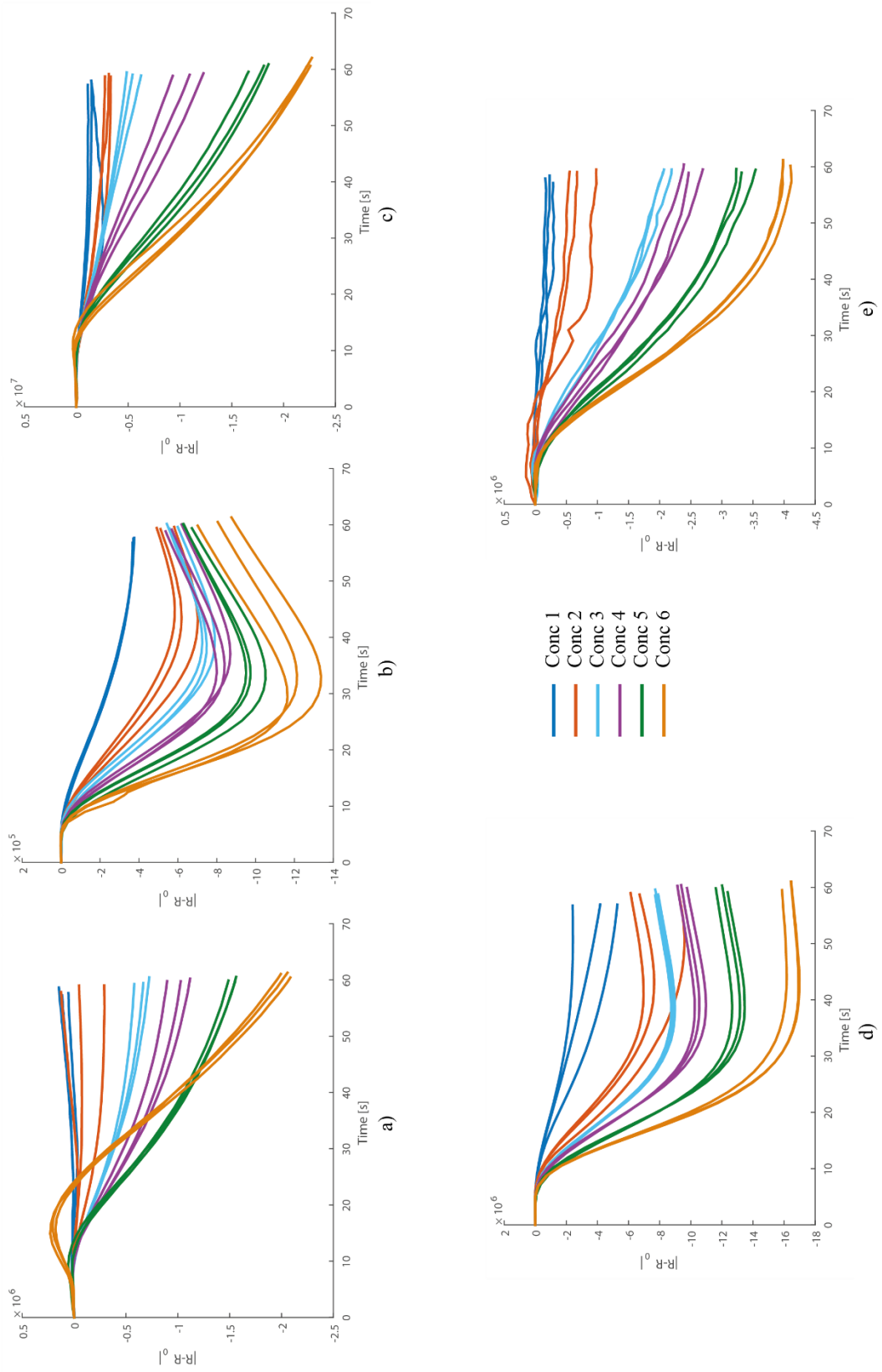

Doi: https://doi.org/10.1016/j.jallcom.2016.09.125

Figure 6

Doi: https://doi.org/10.1016/j.jallcom.2016.09.125

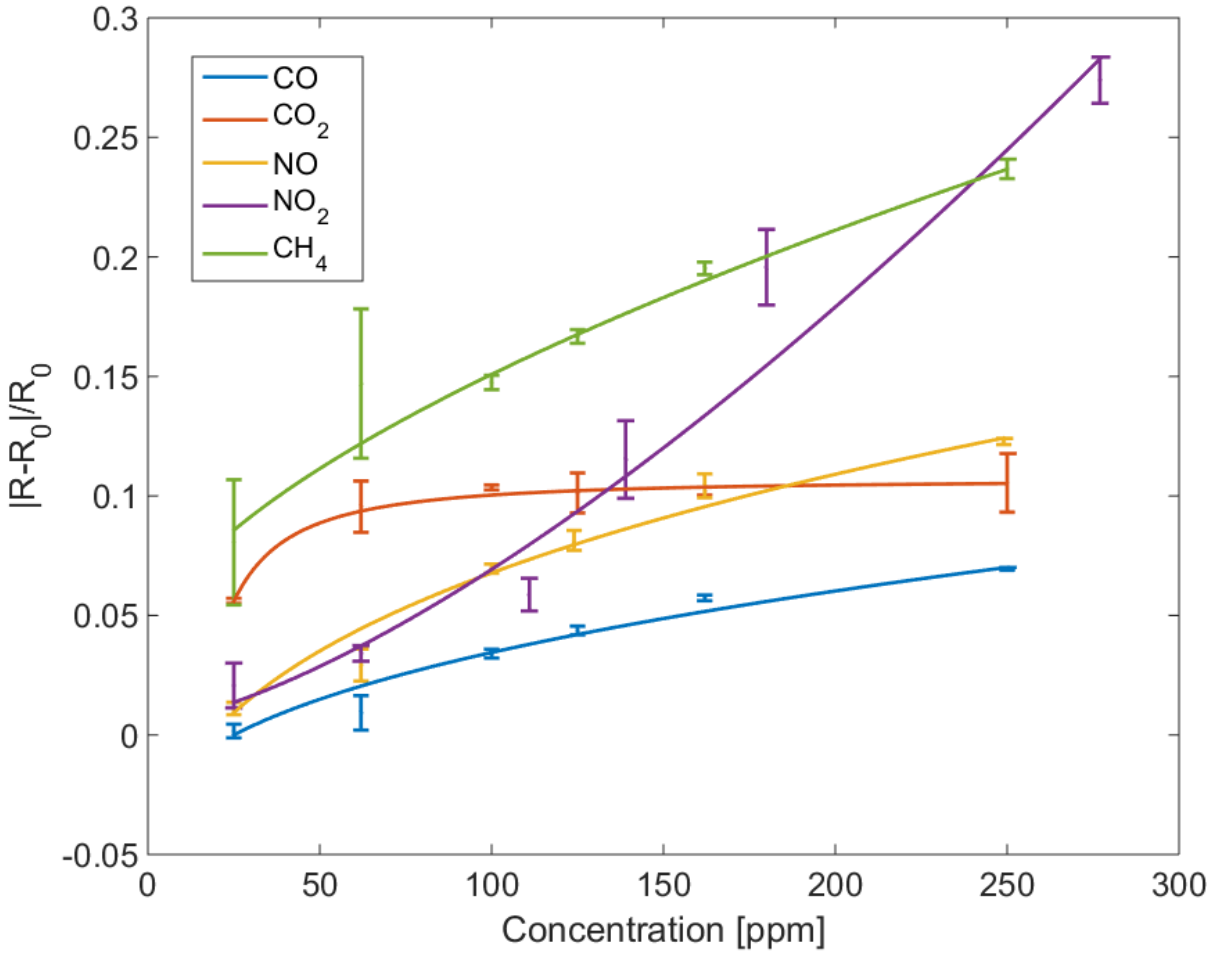

Figure 7

Doi: https://doi.org/10.1016/j.jallcom.2016.09.125

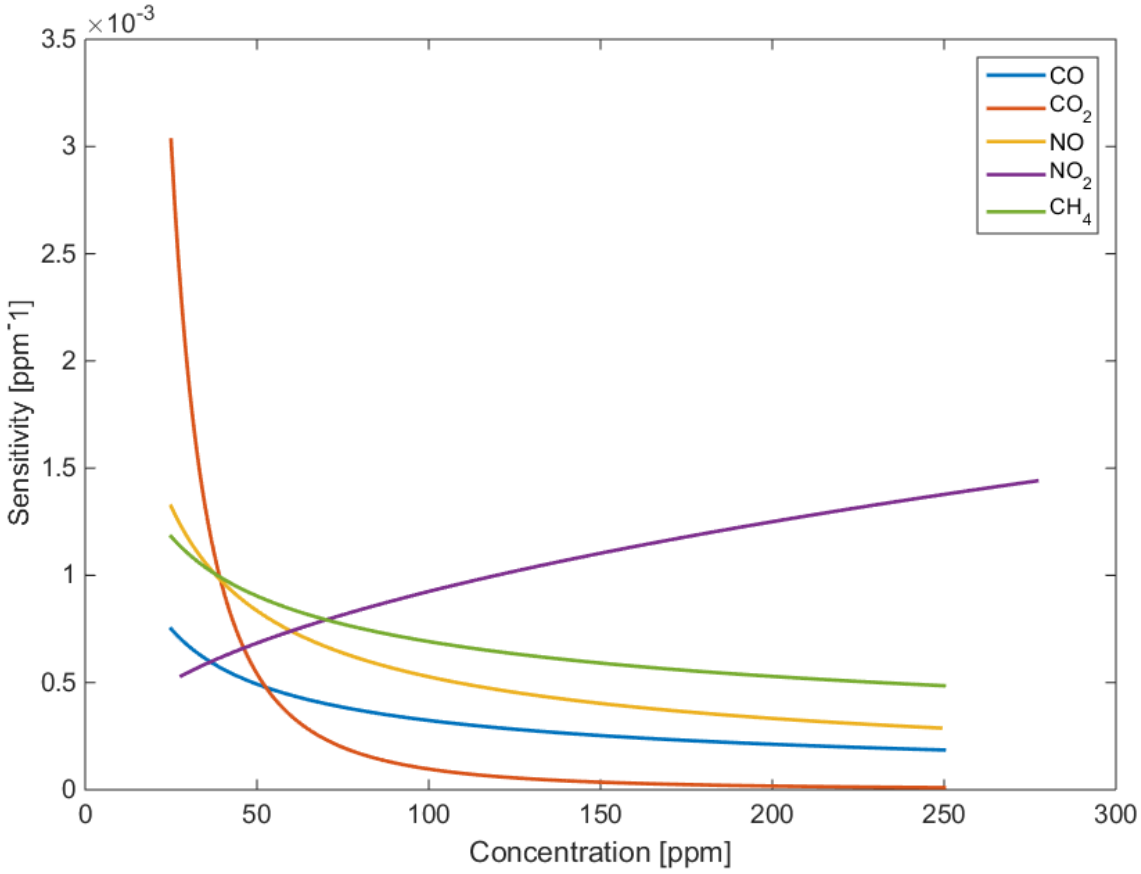

Figure 8

Doi: https://doi.org/10.1016/j.jallcom.2016.09.125

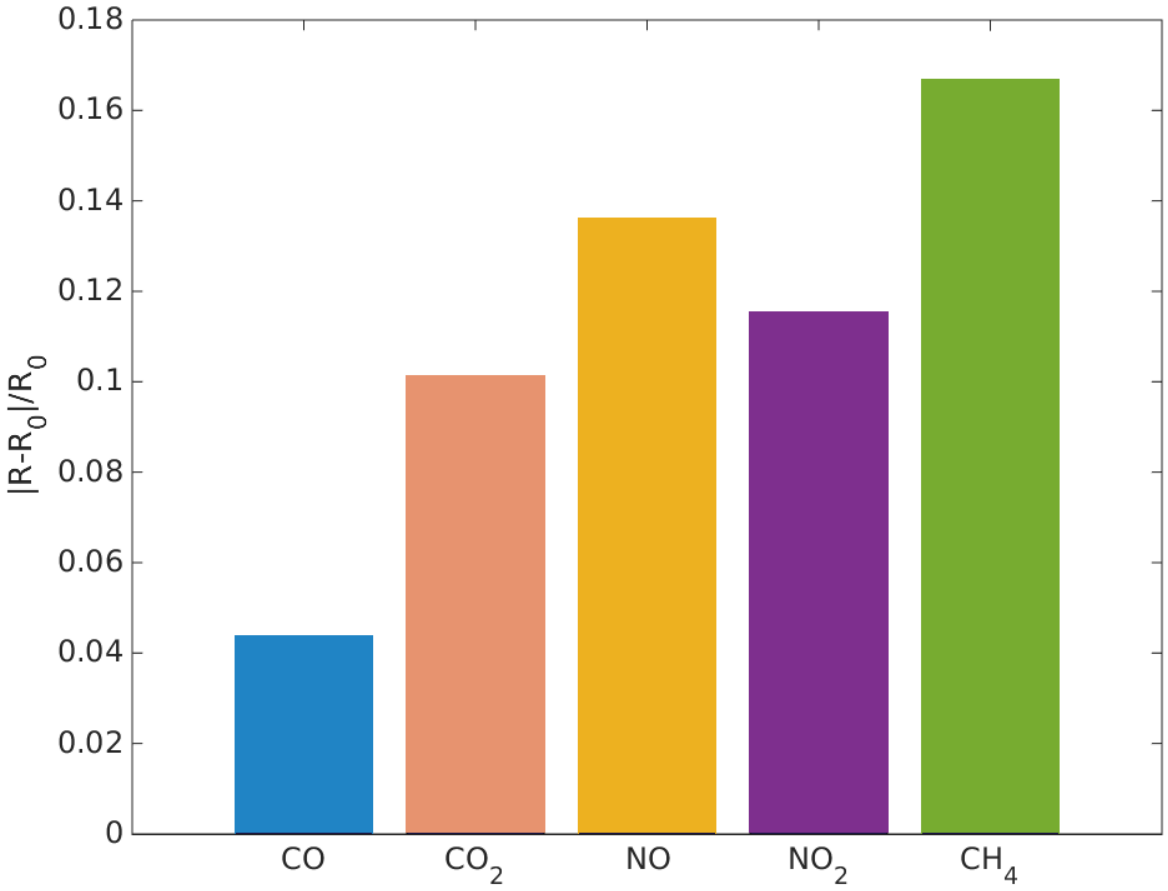

Figure 9

Doi: https://doi.org/10.1016/j.jallcom.2016.09.125

Table 1

Element	Weight [%]	Atomic [%]
O K	20.62	45.69
Al K	8.28	10.87
Cl K	10.68	10.68
Zn L	60.42	32.77
Total	100.00	

Table 2

	CO [ppm]	CO_2[ppm]	NO [ppm]	NO_2[ppm]	CH_4 [ppm]
Conc 1	25	25	25	28	25
Conc 2	62	62	62	69	62
Conc 3	100	100	100	111	100
Conc 4	125	125	124	139	125
Conc 5	162	162	162	180	162
Conc 6	250	250	249	277	250

Table 3

Compound		CO	CO_2	NO	NO_2	CH_4
Fitting	a	0.01348	-6.093	0.03339	8.693e-05	0.006751
	b	0.3926	-1.486	0.3363	1.435	0.6134
	c	-0.0477	0.1069	-0.08936	0.004818	0.03702
R^2		0.9414	0.9090	0.9584	0.9446	0.9624

Doi: https://doi.org/10.1016/j.jallcom.2016.09.125